

Fig. 14-1. 3-ring corona morphing toward iridescence with crepuscular rays in cirrocumulus lenticularis over Cheyenne, WY 10 Mar 2025. Jan Curtis.

# Wonders of the Atmosphere Chapter 14: Coronas, Iridescence, and Glories

Started 21 May 2025

# 14.1 Coronas, Glories, Iridescence, and Icarus

Coronas, Glories, and Iridescence, three *Crowning Glories* of the atmosphere's wonders, were conspicuous by their absence in Chapters 12 and 13 even though they often adorn patterned cloud sheets and lenticular clouds. Now, we give them their due.



Fig. 14-2. A corona in cellular altocumulus, over Cheyenne, WY 29 Aug 2016. Jan Curtis.

First, a correction of a classical Greek myth with words of caution that may save your eyes. One crucial detail is wrong in the myth of Icarus. Daedalus and his son, Icarus were imprisoned in the labyrinth (likely the foundational ruins of the Palace at Knossos) that Daedalus, symbol of the scientific and inventive mind, had designed.

To escape the labyrinth Daedalus designed wings. The next point is where the myth is wrong. Daedalus never would have warned Icarus not to fly too close to the Sun because he knew the Sun is too far away. The warning he gave Icarus was to avoid *looking* too close to the Sun, which would blind him.

On the day of their escape, Daedalus saw lenticular mountain wave clouds in the sky. He knew this meant there were coronas, iridescence, glories, and updrafts, the last which meant excellent soaring weather. You would barely have to flap your wings.

They took off and soon were high above the labyrinth. Icarus looked up at the nearest lenticular cloud to locate the updraft and saw it gleaming iridescent. Looking too close to the Sun, a corona blinded him. Disoriented, Icarus got caught in the turbulent rotor, which shredded his wings. Meanwhile, Daedalus soared above the lenticular clouds, looked down and saw a glory around his shadow on the cloud below and watched bereft as his son plunged into the sea.

At their best, coronas, iridescence, and glories are among the most colorful atmospheric optical phenomena, as in both frames of Fig. 14-1. All are produced when tiny droplets, ice, and other particles, though usually droplets scatter sunlight or moonlight. In general, the largest particles produce the smallest coronas and glories. Iridescence, which spreads the furthest, is produced by the tiniest droplets, usually at cloud fringes. Particle shape when not spherical, as with pollen grains, affects the shape of coronas.

Coronas are small, concentric, and for the most part, more or less circular rings of light around the Sun or Moon that follow a more or less standard color sequence. The aureole is the innermost and brightest part of the corona and the part seen most often, as in Fig. 14-2. It consists of a blindingly bright bluish-white core surrounded by a yellow ring that grades outward to red. For cloud droplets with  $r_{\rm DROP} > \approx 5$  µm, the outer red part of the aureole only extends < 5° from the Sun. Therefore, coronas must be viewed with great caution, blocking the Sun with some object or with your extended hand, and viewing them through dark sun glasses. Even with the Sun blocked by the seat of a ferris wheel in Fig. 14-3, the corona's inner aureole was blindingly bright.



Fig. 14-3. Corona aureole with iridescence in streaks parallel to cloud bands from bottom left to top right, San Mateo, CA, 16 Jun 2016. SDG.

There are other tricks to viewing coronas safely. They can be seen more easily around the Sun's reflection on smooth water or on a car's windshield because the albedo of water is only  $\approx 3\%$  and of glass is only  $\approx 7\%$ . Coronas around the Moon are safe to look at and their colors are easier to see than solar coronas because sunlight is so bright it oversaturates the eye and (often) the camera.

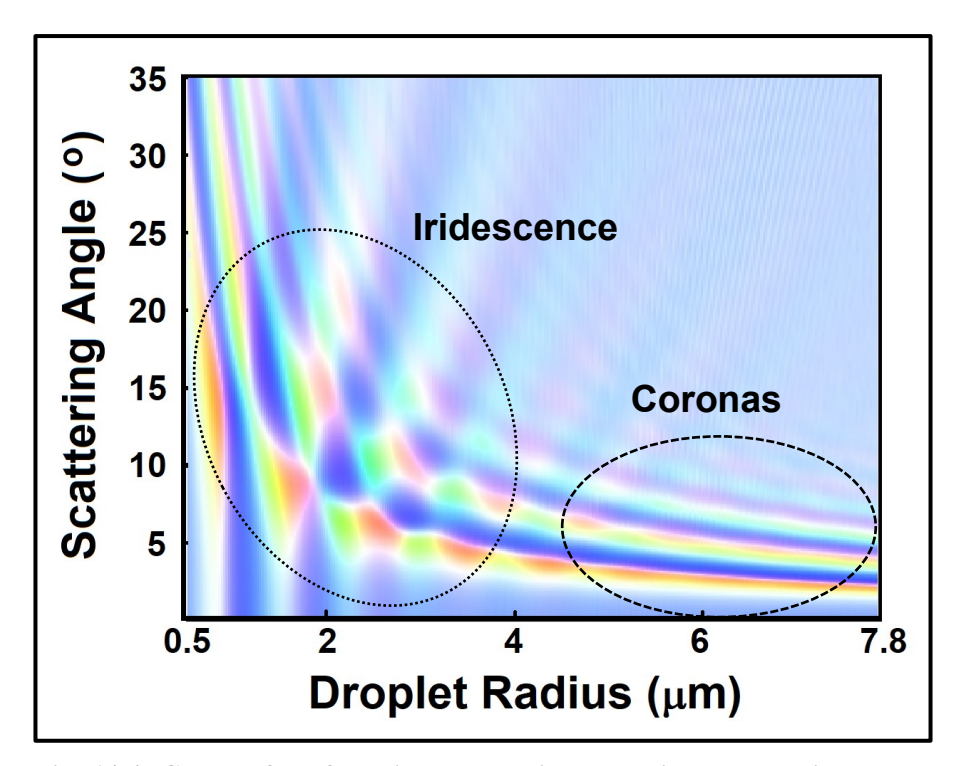


Fig. 14-4. Colors of perfect, single scattering Lee Diagram showing where coronas and iridescence dominate. SDG.

Iridescence is produced by the same scattering process as coronas but differs in shape, tending to follow the fringes of the cloud elements, as in Fig. 14-3 (taken at the San Mateo Fair) where iridescent streaks extend from bottom left to top right parallel to cloud bands outside the aureole of the corona in the central cloud mass. Because droplets are smaller at the cloud fringes, iridescence tends to span a wider angular range of the sky than coronas, sometimes stretching more than 30° from the Sun, where it can be viewed safely. The play of colors is also more irregular, and while often pastel may be more vivid, particularly in some polar stratospheric (nacreous) clouds.

Glories tend to be circular rings around the antisolar point (i. e., the viewer's or camera's shadow). There is no trouble looking at glories. They can be beautifully colored but are never blinding.

# 14.2 Coronas vs Iridescence: Lee Diagram



Fig. 14-5. Corona with 4 rings in cirrostratus translucidus over Cheyenne, WY, 21 Nov 2024. Jan Curtis.

Coronas are often explained in terms of diffraction of light around spherical droplets, but this only works well for  $r_{DROP} > 4$  µm. Mie scattering is needed to explain coronas and iridescence produced by droplets with  $r_{DROP} < 4$  µm, as Jim Lock and Leiming Yang first showed in 1991. Twelve years later, Phil Laven and independently, Stan and Jim Lock simulated coronas and glories photorealistically. Constructing a Lee diagram, much like Fig. 14-4, Laven went on to show the distinction between coronas and iridescence.

Let's decipher the Lee diagram of Fig. 14-4. It is a 'perfect', single Mie scattering model, an ideal few coronas approach. It shows the color of sunlight scattered by a droplet of any size up to  $r_{DROP} = 7.8$  µm and at any angle up to 35° from the Sun. For example, sunlight scattered by an angle of 15° by a droplet with  $r_{DROP} = 2$  µm is purplish red.

Fig. 14-4 does not show irradiance, though the Mie solution includes it. The relative irradiance of the scattered light is highly oscillatory for any wavelngth and radius, and decreases rapidly as scattering angle increases. One example of the Mie solution for relative irradiance as a function of scattering angle is shown for droplets with  $r_{DROP} = 8 \mu m$  as the green curve in Fig. 1-16.



Fig. 14-6. Elliptical corona with three rings and an indentation, Cheyenne, WY 22 Nov 2023. Jan Curtis.

The Lee diagram can be divided into two distinct regimes – the corona regime for  $r_{DROP} > 4 \mu m$  at small scattering angles (the lower right quadrant), where diffraction is an excellent approximation to Mie scattering, and the iridescence regime for  $r_{DROP} < 4 \mu m$  over a wider range of scattering angles. A momentary glance shows that diffraction fails to explain the color pattern of the iridescence regime.



Fig. 14-7. Corona in cirrocumulus translucidus undulatus 31 Mar 2020 over Cheyenne, WY. Jan Curtis.

In the corona regime diffraction is an excellent approximation to Mie scattering. Coronas are 'well behaved', with an angular width that varies inversely with droplet radius. The aureole for  $r_{DROP} = 4 \mu m$  extends 4° from the Sun; the aureole for  $r_{DROP} = 8 \mu m$  extends only 2° from the Sun. In this way, coronas provide casual observers a way to estimate the size of droplets or ice particles in the cloud above.

The corona regime's color pattern is almost constant and is easily extended to droplets larger than  $r_{DROP} = 7.8 \mu m$ . Four or five distinct but progressively fainter cycles of color sequences (blue – yellow – red) occur, although 4-ring coronas, such as the one produced in a translucent sheet of mountain wave cirrostratus over Cheyenne, WY on 21 Nov 2024, are very rare. Even 3-ring coronas are exceptional, such as the corona seen in lee wave-induced cirrostratus through an almost leafless cottonwood tree in Cheyenne, WY on 22 Nov 2023 (Fig. 14-6). But color purity can be as great for a 2-ring corona, as on 31 March 2020, which formed in a gossamer thin rippled



Fig. 14-8. Near circular corona produced in altocumulus by a full Moon 25 Feb 2021 over Cheyenne, WY. Corona is blotted out where cloud is optically thick at lower right. Jan Curtis.

cirrocumulus translucidas undulatus (Fig. 14-7), also a lee wave cloud.

Coronas are circular only if the droplet size spectrum is constant across a wide enough area of the cloud sheet, as in Fig. 14-2 and in the corona around the full Moon over Cheyenne, NM on 25 Feb 2021 (Fig.14-8). If the cloud has a gradual horizontal gradient of mean droplet size, elliptical coronas result, as in Fig. 14-6. The indentation of that corona extending to the upper left indicates larger droplet sizes, likely where air rose in the crest of a wave in the cloud.



Fig. 14-9. Distorted corona with iridescence in altocumulus lenticularis translucidas 18 Dec 2019 over Cheyenne, WY. Jan Curtis.

Greater distortions in the shapes of coronas occur when droplet sizes vary irregularly over a cloud sheet. Not only is the corona in the right panel of Fig. 14-1 oblong, it also has a large indentation along the crepuscular ray, whose shadow somehow resulted in illumination by larger droplets than elsewhere. Fig. 14-9 contains a highly distorted corona because it traverses several waves in the parent lenticular cloud. Similar fluctuations of distorted coronas appear near the edges of standing lenticular clouds on 10 March 2025, where they are animated in the time lapse video,

 $\underline{https://www.flickr.com/photos/cloud\_spirit/54381993431/in/photostr} \\ \underline{eam/lightbox/}$ 



Fig. 14-10. Iridescence circling lenticular cloud, Cheyenne, WY, 13 Feb 2024. At upper left, corona fragments in cumulus ring the Sun. Jan Curtis.



Fig. 14-11. Iridescence tracing contours of droplet sizes in an altocumulus lenticularis 30 Dec 2019 over Cheyenne, WY. Jan Curtis.

If the gradient of droplet radii in a cloud is large enough it will dominate the resulting pattern of color and light so that it will circle the cloud, tracing the contours of droplet sizes, as in Fig. 14-10. The iridescence regime has a distorted checkerboard pattern of vibrant colors, like one that would be painted by an abstract artist. It is in this regime of tiny droplets or ice particles that the fringes of lenticular clouds (Fig. 14-10 and Fig. 14-11), pileus atop thunderstorms (Fig. 14-12), and the nacreous polar stratospheric clouds (Fig. 14-14 and Fig. 14-15) display fantastical, peacock colors.

The rich colors of the pileus atop the cumulonimbus cloud at the left of the image of Fig. 14-12 in Delray Beach, FL on 31 July 2012 were enhanced because the pileus with its radial gradient of droplet (or ice particle) sizes ringed the Sun almost exactly as a corona would. Comparing the RGB colorimetric analyses (Fig. 14-13) running the half width of the pileus at left of Fig 14-12 to that (Fig. 9-5) of the vivid rainbow at bottom of Fig. 9-4 reveals that under optimal conditions, the color purity of iridescence can equal or exceed that of the brightest primary rainbows!



Fig. 14-12. Iridescent pileus over a thunderstorm at Delray Beach, FL, 31 Jul 2012. ©National News and Pictures, Ken Rotberg.

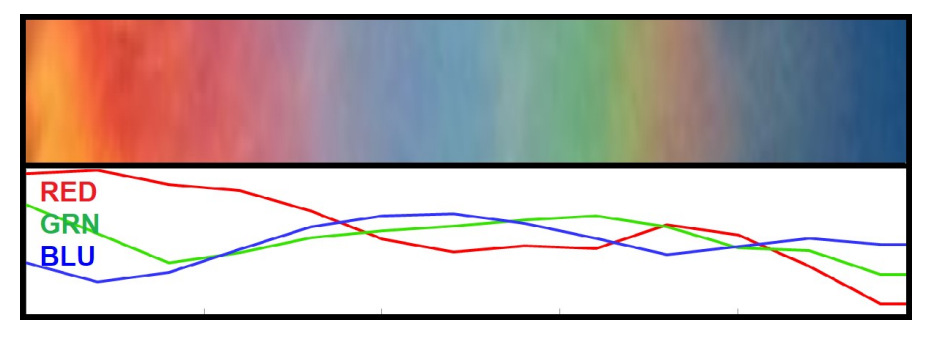


Fig. 14-13. RGB colorimetric analysis of the iridescent pileus at left of Fig. 14-12. SDG.

The iridescent displays of the optically tenuous polar stratospheric clouds only light up in twilight when the troposphere lies darkened in the Earth's shadow and when the near horizontal path through the clouds increases the effective optical thickness. They are produced in



Fig. 14-14. Nacreous cloud over Norway. Video at <a href="https://www.reddit.com/r/Damnthatsinteresting/comments/19dss5e/n">https://www.reddit.com/r/Damnthatsinteresting/comments/19dss5e/n</a> orway mother of pearl clouds also known as/

wave clouds at  $T < -85^{\circ}$ C that consist of near-spherical ice particles with  $r_{ICE} \approx 5$  µm and smaller at cloud fringes, which puts their displays mostly in the iridescence regime of the Lee diagram. Ice

particles, sometimes frozen cloud droplets, also dominate in the iridescent clouds in the upper troposphere, where typically T < -50°C. The brilliance of all these displays, like that of opals, varies from pale to fiery, and depends on the distribution of particle sizes.



Fig. 14-15. Nacreous cloud over Fairbanks, AK late 1990's. Jan Curtis.

# 14.3 Limiting Factors for Coronas

The photographs of coronas and iridescence presented in the last section are not by any means typical. Very few coronas and iridescence approach the color purity of these photos or certainly of the perfect scattering Lee diagram. This is due to three main factors. 1: The particles: As light passes through clouds it encounters droplets or ice particles with a range of sizes. Because scattering angles vary with wavelength and with droplet size, interference almost invariably washes out the colors. It is largely for this reason that most coronas consist only of the aureole. 2: Optically thin clouds ( $\tau_{CLD} \le 0.005$ ) have too few droplets to scatter enough light while multiple scattering washes out coronas in optically thick clouds ( $\tau_{CLD} > 2$ ). Much as with halos, coronas and iridescence have maximum lighting contrast and color purity for clouds of optical thickness,  $\tau_{CLD}$  = O(0.1), As  $\tau_{CLD}$  increases, so do the corona-impairing effects of multiple scattering and the range of droplet sizes. 3: Skylight adds a blue tint, but mainly for iridescence at large scattering angles.

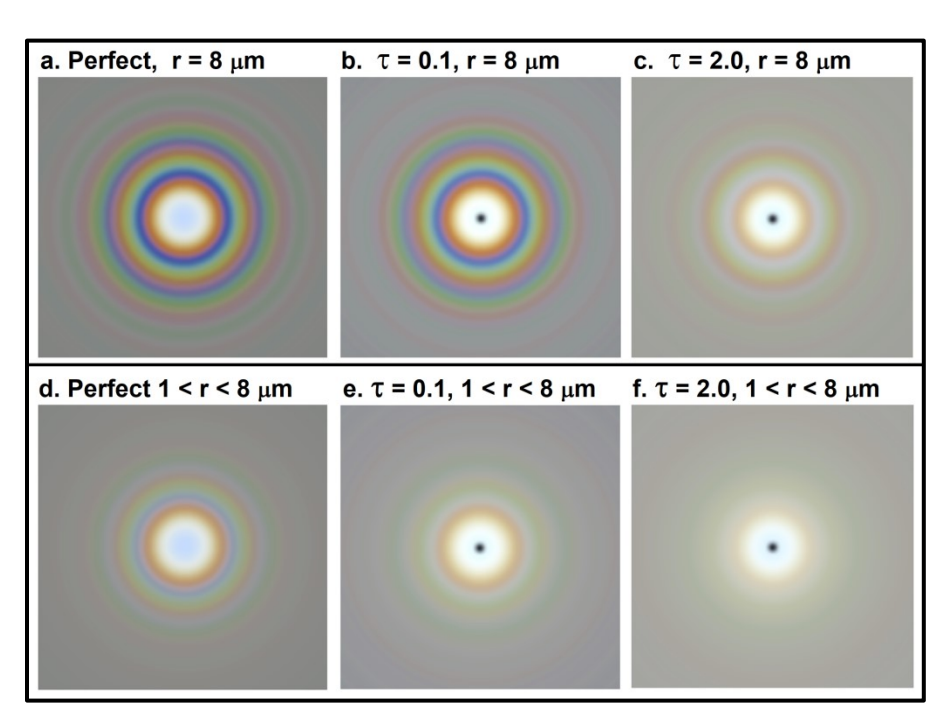


Fig. 14-16. Simulated coronas for perfect single scattering and cloud optical thicknesses,  $\tau = 0.1$  and  $\tau = 2.0$  for droplets with r = 8 µm (top row) and a wide, constant distribution from 1 < r < 8 µm. SDG

The corona simulations in Fig 14-16 (using Mie scattering) show how severely broadening the droplet size spectrum and including scattering in clouds of finite optical thickness reduces the color purity of coronas. Coronas approach the theoretical limit when all droplets are the same size and the cloud is optically thin. Color purity decreases markedly (due to interference) with a wide spread of droplet sizes, in a manner equivalent to diminishing the value of an opal from \$100,000 to \$100. Increasing optical thickness to  $\tau = 2$  reduces color purity and brightness markedly, even when all droplets are the same size. For a wide spread of droplet sizes all that remains is the aureole. Increasing cloud optical thickness to  $\tau = 4$  leaves but a faded aureole.

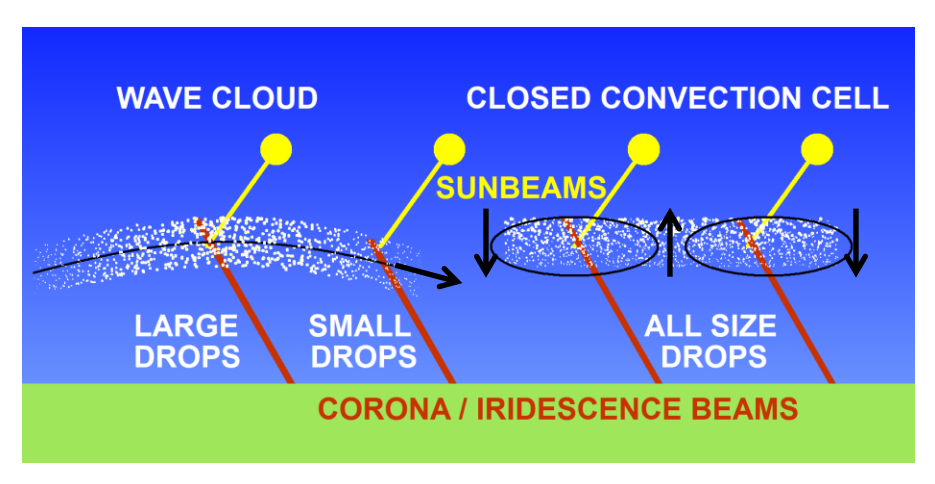


Fig. 14-17. Narrower drop size distributions along beam give wave clouds more colorful coronas and iridescence than convective clouds. SDG

As the photographs in this section suggest, and observations confirm, lenticular wave clouds produce some of the most vivid coronas and especially iridescence. Similarly, altocumulus and cirrocumulus consisting of fine ripples (undulatus) produce more vivid coronas and iridescence than those composed of polygonal convection cells. The main reason for this, illustrated in Fig. 14-17, is that the corona / iridescent beams (red lines) encounter a much smaller range of droplet (or ice particle) sizes from top to bottom through wave clouds than through convective clouds. In convection cells, air rises almost vertically so droplet sizes range from zero at cloud base to a maximum at cloud top. The result is that corona / iridescent beams encounter a full range of droplet sizes as they pass through convection cells. In wave clouds, droplet size, and usually optical thickness as well, increase horizontally from tiny values at cloud fringe to maxima at the wave crest. This horizontal segregation of droplet sizes in wave clouds means that corona / iridescent beams passing through the fringes encounter tiny droplets of almost constant size, while corona / iridescent beams passing through the crests encounter larger droplets of reasonably uniform size provided the cloud is optically thin. If the cloud is optically thick in center it will be white or gray from multiple scattering.

Uniform fields of optically thin cellular Altocumulus cloud sheets are more likely than wave clouds to produce circular coronas, but seldom with vivid colors and multiple rings unless wave activity is involved, particularly when wind shear orients the cells in ranks and rows.

#### 14.4 Pollen Coronas

It's spring. You are feeling poorly. Your nose is running and your eyes are watery. The sky seems to be clear but you are pretty sure you see a small, odd-shaped corona around the Sun. You are right. The pollen that disturbs you disturbs sunlight too.



Fig. 14-18. Pollen coronas from alder trees (left and center ) and birch (right). ©Jari Piikki.

In the spring of 1989, Finnish observers of the Ursa Astronomical Association noticed odd-shaped coronas in clear, cloudless skies (Fig. 14-18). But the clear sky was tainted with tiny pollen grains from the surrounding forests.

Pollen grains can produce bright, vibrant coronas because the grains of particular species of tree are all close in size and shape and therefore diffract light coherently. But pollen coronas are not circular because pollen grains are not spheres. Alder pollen is ridged and

oblate (flattened) (20 $\mu$ m high and 25  $\mu$ m wide). Birch pollen is slightly elliptical, with 3 small lobes (30–35  $\mu$ m), while pine and

spruce pollen (50–>75 μm) resemble Mickey a round body and two bladders that resemble large ears (Fig. 14-19). Since non-spherical pollen grains fall so that the widest side is almost horizontal, alder and birch



Fig. 14-19. Ponderosa pine pollen. Rocky Mountain National Park.

pollen produce elliptical coronas that are higher than wide and pine pollen produces coronas with polygonal lobes (Fig. 14-19).



Fig. 14-20. Glory and fog bow from the Golden Gate Bridge, 13 Jul 2007. ©Mila Zinkova.

# **14.5 Viewing Glories**

The first time that members of the scientific expedition to Peru saw the Sun rise on the summit of Pambamarca (now Ecuador) perhaps in 1737, they noted with "boundless astonishment" three concentric rainbow-like rings around the shadow of their heads surrounded by a much larger whitish ring, all on the thin mist no more than 20 steps away. Antonio Ulloa and Pierre Bouguer, much less conceited and more scientific than Benvenuto Cellini, found that as they moved from side to side the apparition moved with each of them, but what was most impressive was they noted that each of the six or seven other people saw the apparition only around their own shadows.

What they saw, illustrated, and measured was the multi-ringed, colored glory and the near white cloud bow. They found the inner ring and the cloud bow extended about 2.75° and 33.5° respectively from their shadows.



Fig. 14-21. Multi-ringed glory with rainbow colors inside a white fog bow atop the Zugspitze 15 Nov 2014. ©Claudia Hinz.

Glories resemble coronas, but appear almost directly opposite the Sun. Glories are rings of light colored like small rainbows that surround an observer's shadow on a cloud deck or fog bank. Before the age of powered flight, glories were seldom seen but were (as just

noted) described in almost ecstatic terms by mountaineers and balloonists. Now that planes fly above clouds, glories have almost become mundane. The next time you fly, look down at the shadow of the plane on the clouds below and you will probably see a glory surrounding it. Yet the glories seen from high-flying jets far above the cloud decks below rarely are bright and colorful enough to evoke much excitement. In many cases they are surrounded by cloudbows so faint, broad, and colorless that they are only detected by a trained eye.



Fig. 14-22. Glory around the shadow of a jet. ©Stephen James O'Meara.

All the best sightings and photos of glories occur when the observer is very near the cloud or mist. Knowing this, Mila Zinkova perched herself on the walkway of the Golden Gate Bridge, where a long tongue of fog often pours through the Gate. She came on many late afternoons when the western Sun was low enough in the sky for a photo op should the top of the fog pass under the walkway so that she could see the Sun shine on it. And that is how she was able to take the photo in Fig. 14-20. Note that whitecaps can be seen below.



Fig. 14-23. 3-ring Glory near sunset. Stan does not fly First Class. SDG

Claudia Hinz (whom we have already met in Chapter 11 through her mountaintop photos of halos) also positioned herself perfectly to capture glories and fogbows atop several peaks including the Zugspitze (Fig. 14-21), which, because of its greater height, produced the best and most frequent glories.

From the air, the best views of glories occur when the plane is only a short distance above the cloud deck. For the majority of long-distance flights, glories are seldom dramatic because they tend to appear in cloud decks far below flight level of 11 or 12 km and. That is why on short flights that barely rise above cloud top Alexander Haussmann always reserves a window seat opposite the Sun. Glory seekers including Phil Laven and Stephen James O'Meara (Fig. 14-22), know when to reserve seats facing away from the Sun (but never over the wing) and know to be ready the moment the jet rises above a cloud layer (Fig 14-23) or is about to descend into one.

A standing joke, based on the fact that the glory is centered around the photographer's shadow and almost all glory photos are centered in the middle or back of the planes, is that glory afficiados seldom fly first class.



Fig. 14-24. Striped glory SW of Guadalupe Island and von Karman vortices aligning cloud cells in the island's wake, 20 May 2008. NASA MODIS TERRA.

Glories are even seen from space, though they are seldom dramatic, even after intervening skylight has been removed by processing, as in NASA MODIS images (Fig. 14-24). These images occasionally capture glories when the Sun is near the zenith above the decks of stratocumulus over the subtropical oceans. The best 'MODIS' glories occur when the deck consists of fine, almost translucent cells. The

'MODIS' glories always appear as two parallel multicolored stripes because the satellite sensors sweep back and forth, east and west as they circle the globe, capturing narrow bands that are stitched together to form coherent images. Note that the glory stripes in Fig. 14-24 are brightest and most colorful where the cloud cells are very thin and disappear where they are optically thick and bright white.

# 14.6 Modeling Glories: Lee Diagram

A simple physical explanation for the glory remains elusive. The closest we have come to solving the mystery of the glory is that it appears to be due in good part to light that strikes cloud droplets and skirts around their surfaces before scattering almost directly back from the direction it came. The angular size of the glory's rings varies almost, but not exactly, inversely with the size of the drops, so, as with coronas, 1: the largest glories are produced by the smallest droplets and, 2: the best glories are produced when the droplets are almost all the same size to minimize destructive interference.

Even though glories do not seem to be governed by a simple physical principle, they are still modeled accurately using Mie scattering. The Lee diagram of Fig. 14-25 of the perfect single Mie scattering model shows two distinct but overlapping regimes. The glory regime prevails close to the antisolar point for larger droplets and at all angles for small droplets or particles, including and extending somewhat beyond the lower left half of the diagram. These idealized glories include the aureole plus five distinct bands, each successively less saturated and distinct. The bands are large for small droplets and decrease in size as droplet size increases.

The regime of fog / cloud bows also reveals up to five distinct bands, but in contrast with the glory, 1: fog / cloud bows increase in size as droplet size increases and, 2: the most distinct fog / cloud bows occur furthest from the antisolar point. As a result, the overlapping region of glories and fog/cloud bows always appears indistinct, even in the

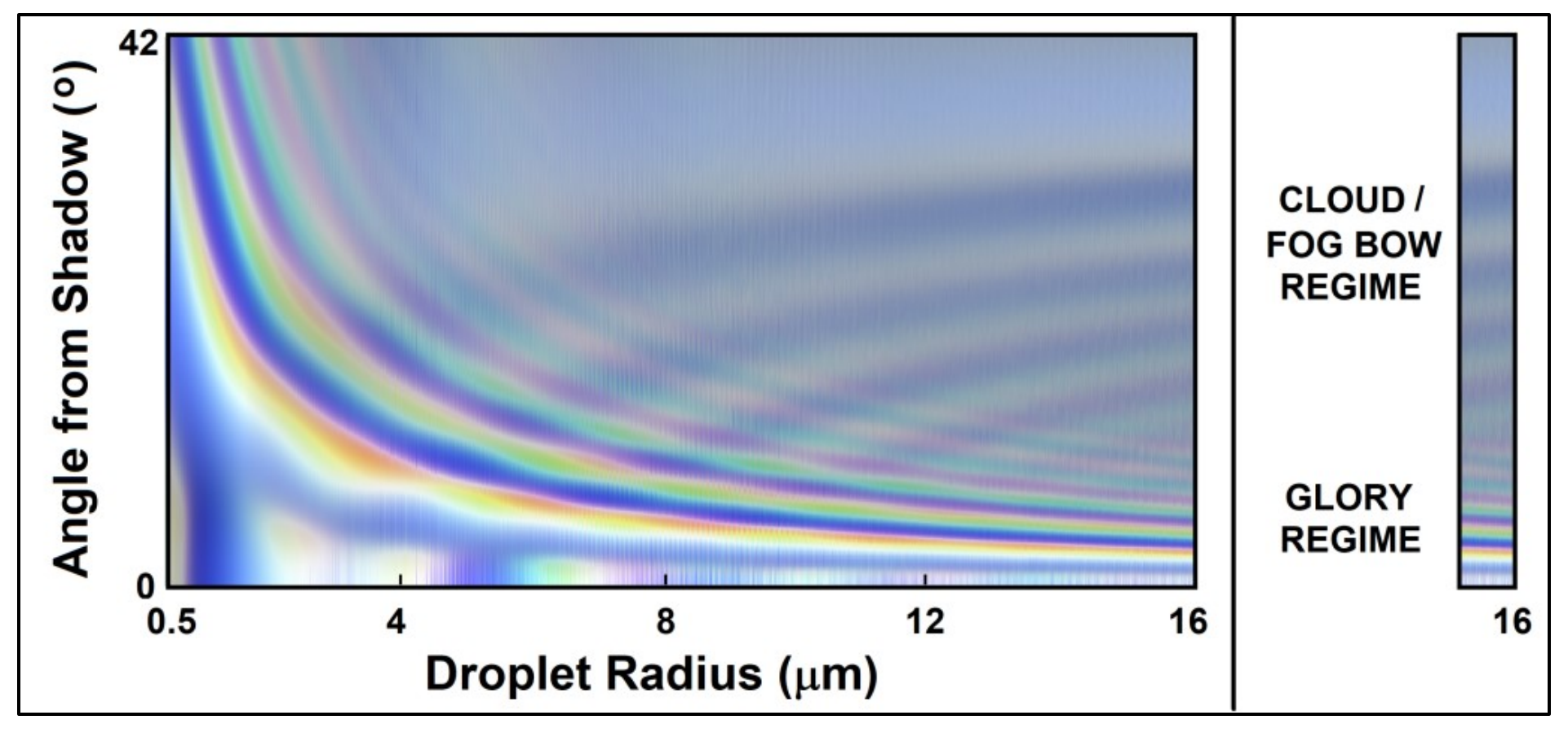


Fig. 14-25. Lee diagram of perfect single Mie scattering for regimes of glories (bands tilting down to the right) and of cloud / fog bows (bands tilting up to the right) as a function of droplet size and scattering angle from the shadow (antisolar point). Extract at right shows the change of regimes for  $r_{DROP} \approx 16 \,\mu m$ . SDG.

most superlative sightings and photos, for example atop the Zugspitze on 13 Jan 2013 (Fig. 14-26).

Glories always fall far short of the theoretical maxima of brightness and color purity given by perfect, single Mie scattering theory for a single particle. Glories suffer the same limitations of brightness and color purity as do rainbows, halos, and coronas. First is the inherent inefficiency of radiative transfer in clouds of particles because many sunbeams pass through optically thin clouds without being scattered, and multiple scattering vitiates all optical phenomena in optically thick clouds. The result is that the maximum possible scattering

efficiency equals  $e^{-1} \approx 36.8\%$ , which occurs when optical thickness,  $\tau_{\text{CLD}} = 1$ , but only in a cloud with all particles the exact same size and shape. Interference further reduces peaks of color purity and brightness, and may obliterate the outer rings whenever there is a broad drop size distribution, as is the case in most clouds. Under such conditions, the glory is reduced to a bright, inner pale yellow ring and a single red ring. The inner blue ring of glories is seldom distinctly visible even if outer red rings can be seen. The blue ring is easily washed out by interference caused by a drop size distribution because it occurs in a brightness minimum.



Fig. 14-26. Multi-ringed glory and fog / cloud bow atop the Zugspitze on 13 Jan 2013. ©Claudia Hinz.

Skylight of the foreground and background, and reflected light from the ground further vitiate the visual contrast of glories. Foreground skylight between observers flying at jet stream levels and the top of a stratocumulus cloud deck over the subtropical oceans is several times brighter than the glory beam. No wonder, glories stand out best when the observer is located near the cloud and when the background is dark and nearby.

The color purity and distinctness of the glory rings are also impaired by the Sun's finite angular width, particularly for droplets larger than  $r_{DROP} > 20$  mm because the rings are only a few times wider than the

Sun. We have seen that this is also the case with rainbows, halos, and coronas.

The simulated glories in Fig. 14-27 (which do not include scattering in the clear atmosphere) illustrate the impact of multiple scattering, cloud optical thickness, and droplet size variation. The left panel shows the perfect single Mie scattering solution for droplets with radius,  $r_D = 4 \mu m$ . In this perfect case, the glory's multiple rings are colorful and extend out to the regime of the cloud bow about 40° from the Sun. The next panel illustrates how much multiple scattering in a cloud of near optical thickness ( $\tau_{CLD} = 0.5$ ) fades the

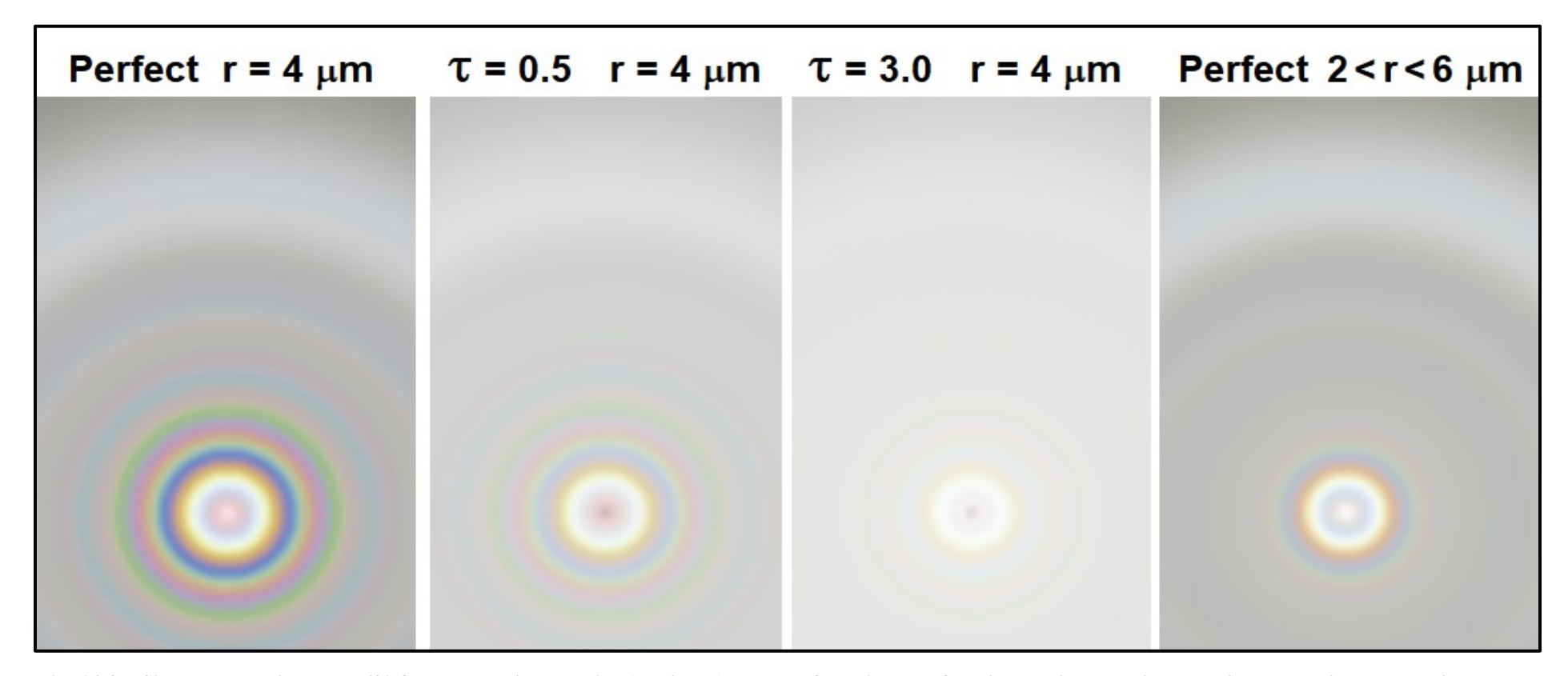


Fig. 14-27. Simulated glories up to 60° from the antisolar point (vertically). From left to right Perfect single Mie scattering: multiple scattering model with  $\tau_{CLD} = 0.5$  and 3.0 in a cloud of droplets with  $r_{CLD} = 4$  µm, and: Perfect single Mie scattering model with a spread of droplet sizes given inn text. SDG.

glory's color purity and brilliance and renders the fog bow faint. When cloud optical thickness is increased to  $\tau_{CLD} = 3$ , the background cloud light overwhelms all but the aureole. Finally, the far right frame shows how greatly a spread of droplet sizes with radii that range in size from,  $2 \mu m \le r_D \le 6 \mu m$ , impair the color purity and brilliance of the glory, leaving only one distinct ring, even for perfect single scattering.

The fact that on occasion glories (and coronas and iridescence) are so bright and colorful despite these potentially crippling limitations makes them all the more marvelous to behold.

#### 14.7 Iridescent Contrails

The vast majority of contrails that criss-cross the sky during the day appear white, in part because they are seen from a great distance and in part because the long-lasting contrails form in the turbulent flow of the moisture-charged jet exhaust (§10.1). Right behind the jet, the shorter-lived contrails of uniformly tiny droplets or ice particles that form in the laminar flow over the wing offer a chance of being iridescent if they appear near the Sun.

The best chances to see iridescent contrails without a telescope are therefore for an observer flying just below another jet, as in Fig. 14-28 or for a ground-based observer standing below a jet that is either

taking off or landing, as in Fig. 14-29, or, best of all, for an observer with a window seat above or behind the wing where a thin cloud forms just above the wing.

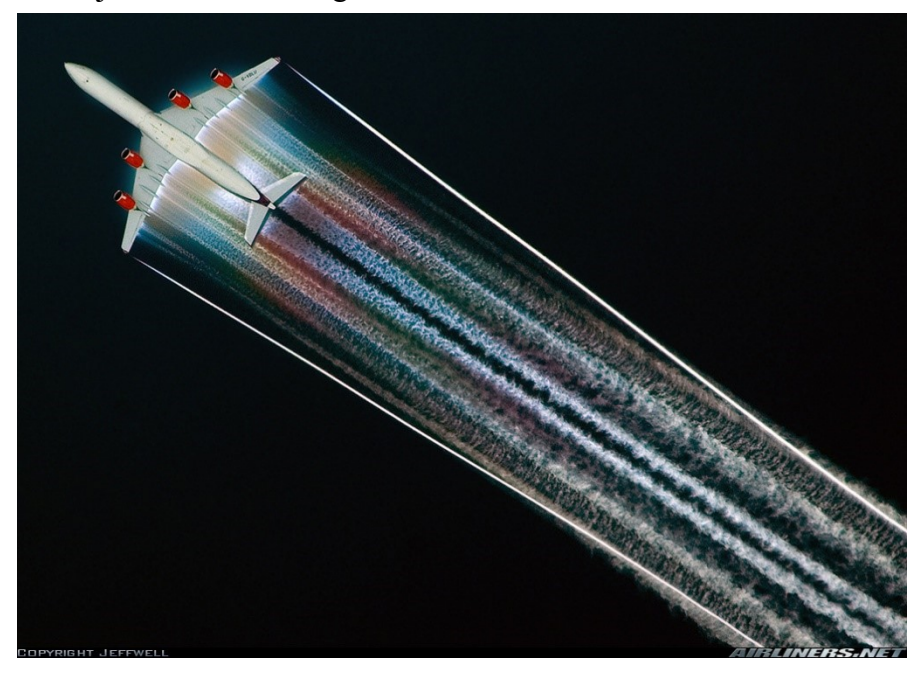


Fig. 14-28. Iridescent contrail made by ice crystals 24 Jul 2006 Jet at 9600 m over Chinaand seen from another high-flying jet. ©Jeffwell.



Fig. 14-29. Iridescent contrail made by jet coming in to land at Vienna Airport. © Franz Kerschbaum.